Check for updates

Nordic Hydrology, 29 (4/5), 1998, 347-360

No part may be reproduced by any process without complete reference

Contributions of Snow to the Annual Water Balance in Moshiri Watershed, Northern Hokkaido, Japan

Paper presented at the 11th Northern Res. Basins Symposium/Workshop
Prudhoe Bay to Fairbanks, Alaska, USA – Aug. 18-22, 1997

N. Ishikawa, H. Nakabayashi, Y. Ishii, and Y. Kodama
Institute of Low Temperature Science, Hokkaido University,
Sapporo, 060, Japan

Characteristics of the water balance were investigated in an experimental watershed where there is a seasonal snow cover. To estimate the basin-wide snowmelt by the heat balance method, seven observation sites were established in the watershed and the dependencies of meteorological parameters on elevation, slope, and forest density were examined. In the snowmelt season, the net radiation and sensible heat flux increased with elevation because of the decrease in forest density, an increase in wind speed, and the temperature inversion phenomenon, which resulted in an increase in the snowmelt rate with elevation. The solid precipitation accounted for 53% of the annual precipitation and snowmelt runoff accounted for 45% of the annual runoff. The runoff/precipitation ratio was 0.75 in the snowmelt season. Evaporation was negligibly small during the winter season, but it increased during the snow-free period. The total water loss due to evaporation was about a quarter of the annual precipitation.

Introduction

In snowy regions, the snow cover plays an important role in the hydrologic regime by storing solid precipitation for long periods. The presence of snow reduces the heat exchange between air and the underlying soil. Also snow is important for water resources because meltwater, which is produced not only at the upper snow surface but also at the bottom of the snow cover, penetrates into the ground and contributes to the runoff. Therefore water deficiencies may be replenished throughout the snow

Downloaded from http://iwaponline.com/hr/article-pdf/29/4-5/347/4827/347.pdf
by guest

cover period. The heat balance is a common method to estimate snowmelt rate and has been discussed in many studies (Price and Colbeck 1976; Ishikawa *et al.* 1986; Harding 1986; Gray and Landine 1988). However, these investigations were made on flat and open sites. To estimate the basin-wide snowmelt precisely is very difficult because the characteristics of the heat balance are quite variable due to the varying topography. These mainly affect the solar radiation, air temperature, and wind speed. It is not realistic to establish many observation sites which cover the entire watershed, so models for estimating the basin-wide heat balance have been proposed (Motoyama 1986; Koike *et al.* 1987). Often watersheds are covered by forests, however, these models do not consider forest effects. Ohta *et al.* (1993) described the snowmelt difference between a forest and an open area and explained its cause by the heat balance. Nakabayashi *et al.* (1996) showed radiative properties in forests during the snowmelt season and presented the relationship between forest density and radiative flux. This paper develops a method for estimating a basin-wide heat balance of snowmelt and describes the water balance of a snow-covered watershed.

Study Sites and Observation Method

The intensive observations of heat balance and water balance were carried out at a small experimental watershed over a whole year from April 1993 to March 1994. The watershed is located in Moshiri Basin, northern Hokkaido, Japan (142° 17' E, 44° 22' N) (Fig. 1), which has an area of 1.3 km^2 and an altitude range of 285 m to 535 m. The general winter climate is characterized by very low air temperatures (the minimum is below -35° C), a deep snow pack (about 2 m) and a long snow cover season (more than six months). Seven fixed observation sites (A-G) were established in and near the watershed for continuous measurements of air temperature, wind speed, water vapor pressure, solar radiation, snow depth, and soil temperature. Sites A and B were located in open and flat places; A was a main meteorological observation site. B was the outlet of the watershed where the runoff measurement was carried out continuously using two different types of weirs (a V-notch sharp-crested weir and a 2 m-wide broad-crested weir). Sites C and E were along a mountain ridge. D was located in a small creek with the same elevation as site C. Site F was the highest point in the watershed and G was in a coniferous (acerate) forest near site A. A 10 m observation mast was placed at each site and equipped with instruments for the measurement of air temperature, humidity, and wind speed at two different heights (3 m and 10 m above the ground surface). Precipitation was measured at sites A and F by rain gauges. Sky view factor and snow depth were measured manually at 11 locations, indicated by an x in Fig. 1. All observation items and instruments are shown in Table 1.

We divided the watershed into 50-m intervals based on the map (in total 2,100

Downloaded from http://iwaponline.com/hr/article-pdf/29/4-5/347/4827/347.pdf
by guest

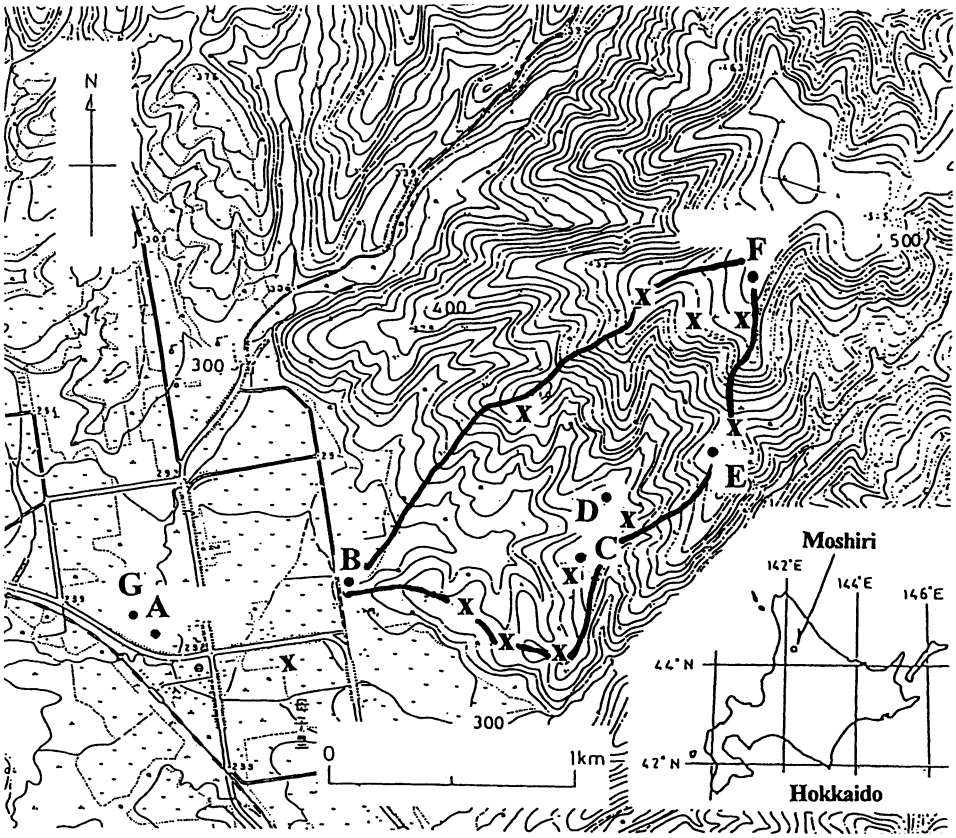

Fig. 1. Experimental watershed of the Moshiri Basin. A, B, C, D, E, F, G: fixed observation sites. X: observation points of forest density and solar radiation

grid points) and obtained the distributions of slope angle and azimuth. Vegetation of the watershed is a mixed forest of coniferous and deciduous trees with an average height of 10 to 16 m. The forest density of the watershed was obtained by using the forest aspect that was constructed by the Office of Uryu-Experimental Forest, Hokkaido University (unpublished). The forest density was defined as the ratio of canopy area per unit area (10,000 m^2) taken from aerial photos. Fig. 2 shows area distributions of forest density with elevation (a), slope azimuth (b), and slope angle (c) of the watershed. The forest density is classified into four groups, such as open (0 to 10%), sparse (10 to 40%), medium (40 to 70%) and dense (70 to 100%). The area below 400 m occupied about 70% of the total area. The open area is about 15%, which is distributed among the upper parts of the watershed. The sparse forest occupies about 60% of the total area and the dense forest occupies the lower part of the watershed. The watershed consists of gentle west-facing slopes, and 65% of the watershed has a slope angle less than 15°.

Downloaded from http://iwaponline.com/hr/article-pdf/29/4-5/347/4827/347.pdf
by guest

Table 1 – Observation items and instruments

Site	items	instruments
A, B, F, G	air temperature	resistance thermometer (ventilation in radiation shelter)
C, D, E	air temperature	resistance thermometer (non ventilation in rad. shelter)
B, C, D, E, F, G	wind speed	three-cup anemometer
A	wind speed	ultra-sonic anemometer
A, B, C, D, E, F, G	solar radiation	pyranometer
A, F, G	net radiation	net radiometer
A, B, C, D, E, F, G	humidity	polymer hygrometer
A, F, G	sensible heat	ultra-sonic anemo-thermometer
B, C, D, E, F	snow depth	optical snow depth meter
A	snow depth	ultra-sonic depth meter
G	snow depth	snow stake
A, F	precipitation	rain gauge
A, B, C, D, E, F	soil temperature	resistance thermometer
A	evaporation	weighing lysimeter
B	runoff	weir

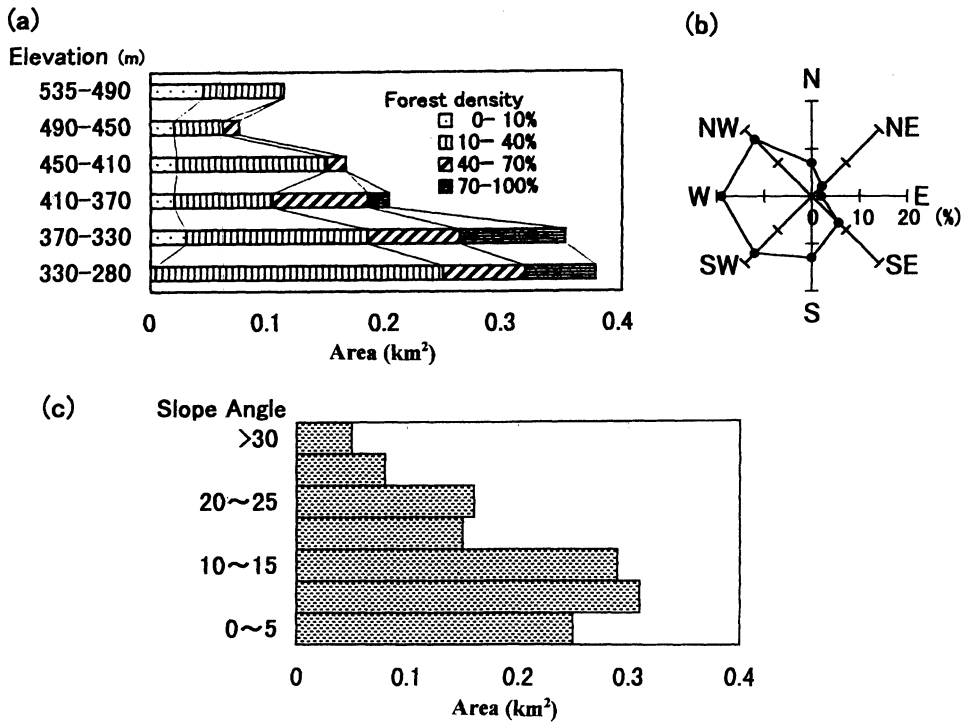

Fig. 2. Area distributions of the watershed (a):forest density, (b): slope azimuth, (c): slope angle.

Downloaded from http://iwaponline.com/hr/article-pdf/29/4-5/347/4827/347.pdf
by guest

Estimations of the Heat Balance on the Snow Surface

Heat balance on a melting snow surface is expressed as follows

$$QH + QE + QN = QM \quad (1)$$

Where QH represents the sensible heat flux, QE the latent heat flux due to evaporation/condensation, QN the net radiation, and QM the heat available for snow. We used the bulk method to evaluate QH and QE, namely

$$QH = \rho_a C_p h \Delta T V_1 \quad (2)$$

$$QE = \rho_a L_e ke \Delta q V_1 \quad (3)$$

Where ρ_a and C_p are the density and specific heat capacity of air; ΔT and Δq are the differences of air temperature and specific humidity at two different heights, respectively; V_1 is the wind speed at Z_1; L_e is the latent heat of vaporization of water; and h and ke are the non-dimensional transfer coefficients for heat and water vapor. QH was obtained directly by using a sonic anemo-thermometer at site A, and was compared with the product of the wind speed and the temperature difference in order to determine the coefficient h. Ishikawa and Kodama (1994b) reported the constant value of h (2.3×10^{-3}) on the melting snow in the range of $0<Ri<0.1$, where Ri is the Richardson Number. It is assumed that under neutral conditions h and ke are the same, following Male and Granger (1981).

In order to obtain the basin-wide snowmelt, the relationships of meteorological parameters with elevation, slope, and forest density of the watershed were examined first.

Dependencies of Meteorological Parameters on Geography

Fig. 3 shows the comparisons of the daily air temperatures at sites A and F from April 1993 to March 1994. Temperatures usually decrease with increasing elevation, but sometimes the opposite tendency appears (the so-called temperature inversion phenomenon). The minimum temperature at site A reached below -30°C but only -15°C at site F. The former observations of air temperatures along the ridge (Ishikawa *et al.* 1994a) showed significant differences between nighttime and daytime vertical temperature profiles: the temperature inversion occurred during the night and the height of the inversion layer was about 380 m (Fig. 4-a), and during the daytime the temperature profile fitted a standard lapse rate condition of 0.6°C/100 m (Fig. 4-b). The air temperatures at any elevation and any time can be estimated from the air temperatures at sites A, C, and F (Fig. 4-b). Both wind speed and water vapor pressure increased with elevation respectively.

Solar radiation on any slope at any time is calculated by the following equation (Oke 1987)

Downloaded from http://iwaponline.com/hr/article-pdf/29/4-5/347/4827/347.pdf
by guest

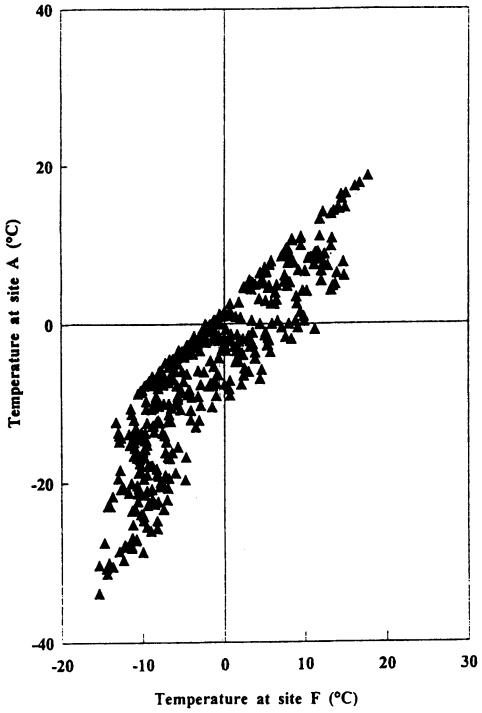

Fig. 3. Comparisons of air temperatures at sites A and F.

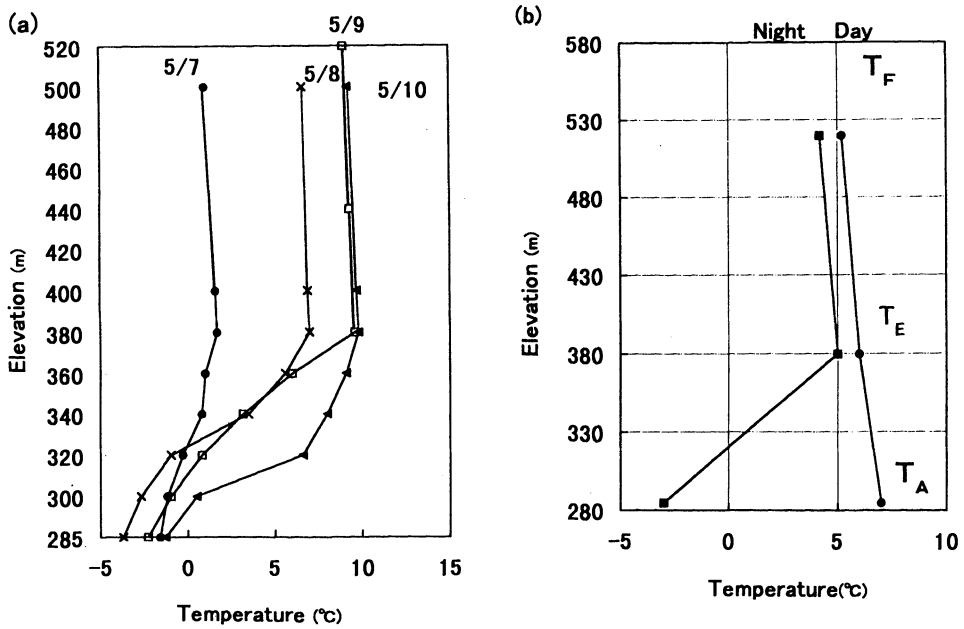

Fig. 4. Measured temperature variation with elevation during inversion and diurnal variation of air temperature of sites A, E, and F.

Downloaded from http://iwaponline.com/hr/article-pdf/29/4-5/347/4827/347.pdf
by guest

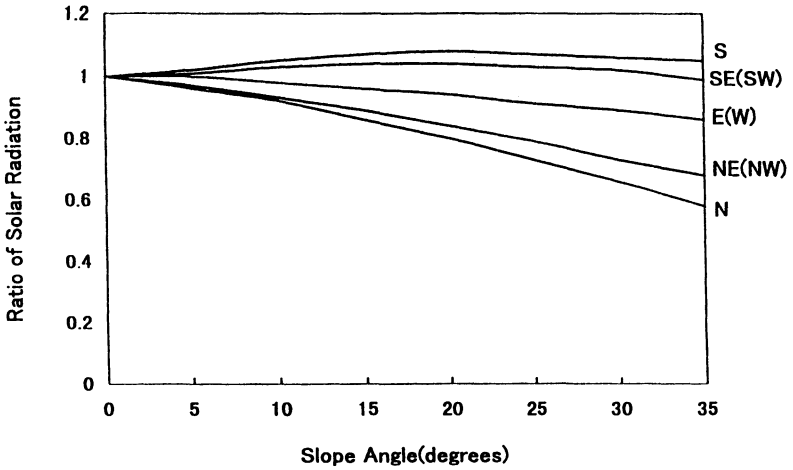

Fig. 5.. Intensity of solar radiation with slope angle and azimuth.

$$D = Do\{\sin Z\cos\theta + \cos Z\sin\theta\cos(A-\beta)\} \quad (4)$$

where Z is the solar elevation, θ is the slope angle, A.is the solar azimuth, β is the slope azimuth, and Do is the direct solar radiation normal to the solar beam. The solar elevation, Z, is expressed by the equation

$$\sin Z = \sin\phi\sin\delta + \cos\phi\cos\delta\cos\varphi \quad (5)$$

Where ϕ is the latitude of an observation site, δ is the solar declination, and φ is the hour angle.

Fig. 5 shows the ratios of the daily direct solar radiation on slopes of differing aspects and angles to the horizontal place at the latitude of 44° N at the end of April (δ = 14°). Southern slopes received more solar radiation and the angle dependency was not clear. Solar radiation on the northern slopes was small and decreased with the increase of the slope angle. The dominant slope of the experimental watershed is a gentle westward slope, so the correction of solar radiation on the slope is small.

Dependencies of Meteorological Parameters on Forest Density

Fig. 6 shows the variations of snowmelt at two adjacent sites A and G for 20 days of the snowmelt season. In early April, only a small difference in snow depth was seen between the two sites. On the other hand the difference became larger during the snowmelt season. The total snowmelt was 90 cm at the open site and 40 cm at the forest site. The larger difference in the snowmelt rate is explained by the comparisons of meteorological features at the two sites. Fig. 7 shows the relationship of the

Downloaded from http://iwaponline.com/hr/article-pdf/29/4-5/347/4827/347.pdf
by guest

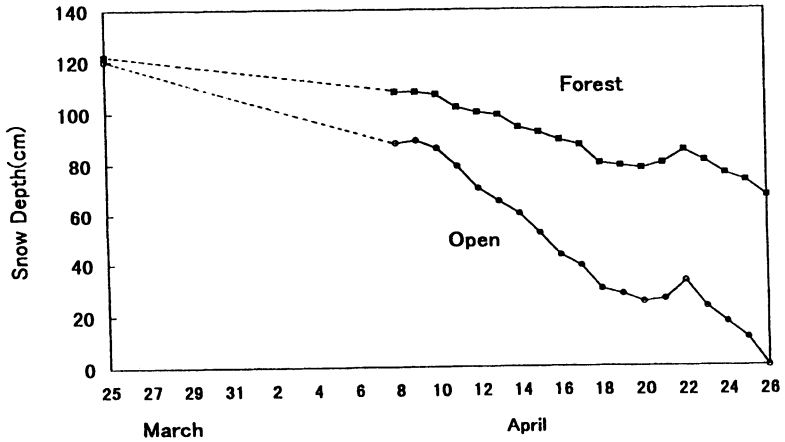

Fig. 6. Comparison of snowmelt at open and forest sites.

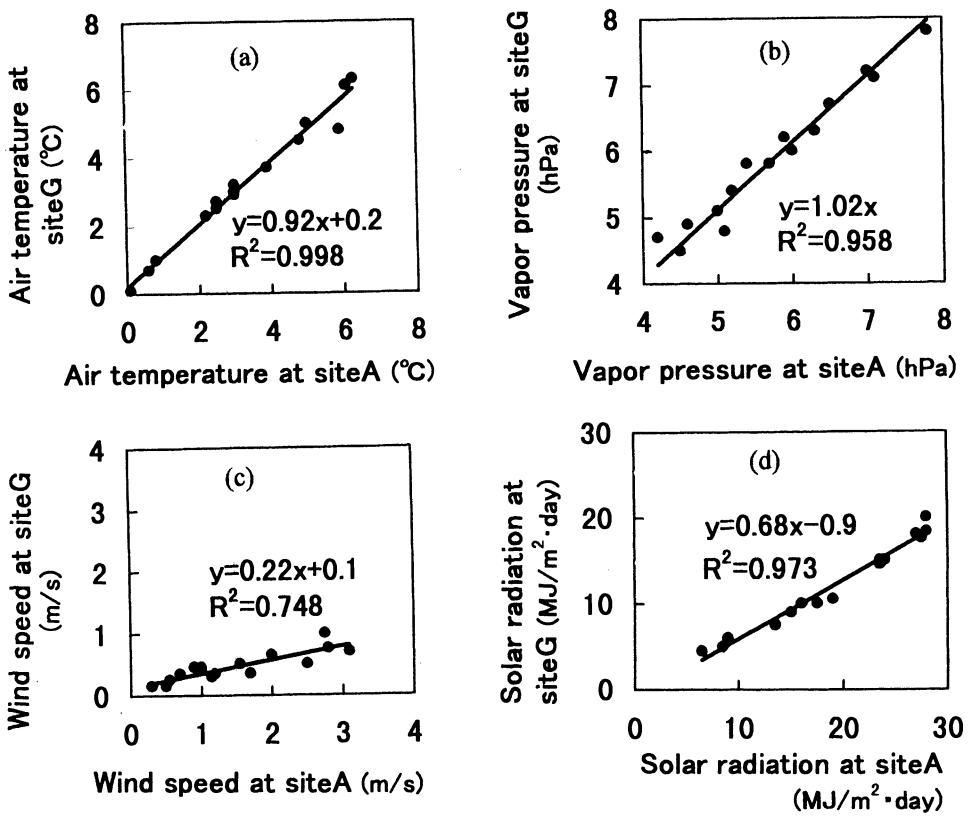

Fig. 7. Comparisons of air temperature (a), vapor pressure (b), wind speed (c) and solar radiation (d) at open and forested sites.

Downloaded from http://iwaponline.com/hr/article-pdf/29/4-5/347/4827/347.pdf
by guest

Table 2 – Ratios of meteorological parameters at the open and forested sites for various forest densities.

forest density	air temp.	vapor press.	wind speed	solar rad.
0-10%	1.0	1.0	0.9	1.0
10-40%	1.0	1.0	0.55	0.95
40-70%	1.0	1.0	0.25	0.8
70-100%	1.0	1.0	0.15	0.6

daily mean of air temperature, water vapor pressure, wind speed, and solar radiation at the two sites during the snowmelt season. Air temperature and vapor pressure show almost no differences at sites A and G, however, the wind speed and solar radiation in the forest were much smaller than at the open site. Site G is located in the dense forest of the watershed. Therefore, we conclude that there are no systematic differences of air temperature and water vapor pressure between the open and forest. However, the influence of the forest on wind speed and solar radiation should be clear. We measured forest density at several points of the watershed by using a camera equipped with a fish-eye lens, and measured the reduction of wind speed and solar radiation at the same points. Table 2 summarizes the ratios of meteorological parameters at an open site and forested sites with various forest densities; all sites are essentially flat.

The net radiation is more important to estimating snowmelt rate than solar radiation, but the net radiation is not commonly measured, so we examined the relationships between solar radiation and net radiation on a clear and on an overcast day (Fig. 8). The values are scattered, but on each day a linear relation was apparent. The net radiation, QN, is expressed by the following equation

$$QN = (1-\alpha)Io + L - \varepsilon\sigma T^4 \qquad (6)$$

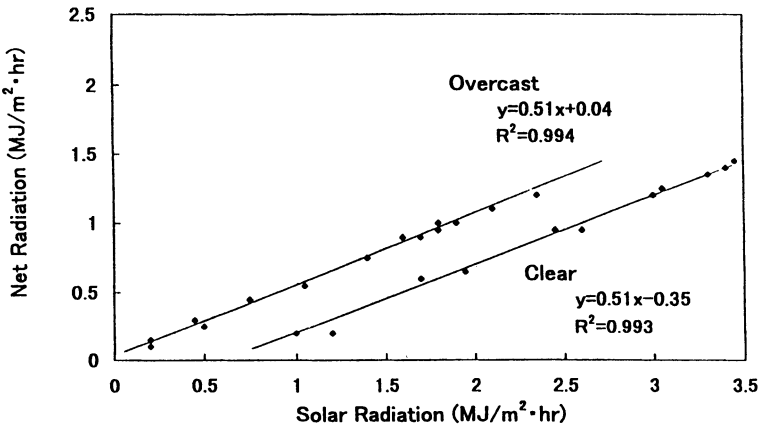

Fig. 8. Relations between solar radiation and net radiation on clear day and overcast day.

Downloaded from http://iwaponline.com/hr/article-pdf/29/4-5/347/4827/347.pdf
by guest

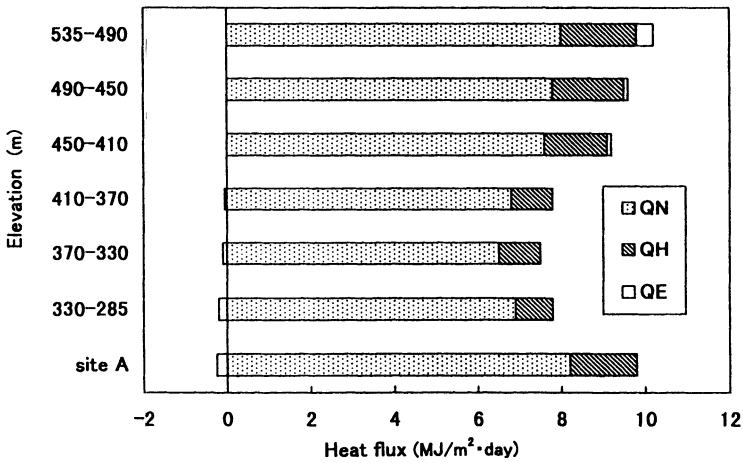

Fig. 9. Snowmelt distributions with elevation. *QN*: net radiation, *QH*: sensible heat, *QE*: latent heat flux due to evaporation.

where α is albedo, ε is emissivity, σ is Stefan-Boltzman constant, L is atmospheric radiation, Io is solar radiation, and T is the surface temperature. The slopes of the lines are 0.51, which shows the albedo of the snow surface is 0.49. Surface albedo was measured in the whole year at site A; it was 0.75 to 0.85 for the dry snow and 0.5 to 0.7 for the wet snow. However, during the intensive snowmelt period the value kept fairly constant: 0.5 to 0.55. Assuming the albedo, emissivity, and surface temperature are constant during snowmelt season, the scatters shown on the figure mean the variability of atmospheric radiation depends in cloud amount C. We obtained the relations

$$\begin{aligned} QN &= 0.51\,Io - 0.35\,(\mathrm{MJ/m^2}) \qquad \text{clear day } (C \leq 10\%) \\ QN &= 0.51\,Io + 0.04\,(\mathrm{MJ/m^2}) \qquad \text{overcast } (C \geq 80\%) \end{aligned} \tag{7}$$

Now the net radiation at any point in the watershed can be calculated once the solar radiation is obtained, considering slope angle and forest density.

The meteorological data at site A (open and flat place) and site F (the highest point) were distributed over the whole watershed, however, topography and forest cover were considered. Fig. 9 shows the mean snowmelt distributions with every 40-m height interval for 10 days. The main energy source is the net radiation, which contributed about 90% of the total snowmelt below 400 m and decreased to 80% above that height. The contribution of sensible heat to the snowmelt increased with elevation because of the decrease in forest density, increase in wind speed, and the temperature inversion. Evaporation occurred at the lower parts of the watershed, but turned to condensation above 400 m. In combination these factors resulted in the snowmelt increase with elevation.

Downloaded from http://iwaponline.com/hr/article-pdf/29/4-5/347/4827/347.pdf
by guest

Water Balance in the Watershed

The water balance of the watershed is expressed by

$$\Delta S = P(\text{or } M) + R + E \quad (8)$$

where P is precipitation, M is snowmelt, R is runoff, E is evaporation, and ΔS is the change in groundwater storage. A positive value of ΔS means recharge of the groundwater storage. Precipitation during the snow-free period was measured at sites A and F, and winter precipitation was obtained by a snow survey at the end of March. Solid precipitation forms seasonal snow cover for a long time and does not contribute to runoff in wintertime. Therefore we split the input of the water balance into two terms: the precipitation during the snow-free season and melt-water in snow cover season. Evaporation from the snow surface was evaluated by the heat balance method at site A, and during the snow-free period it was obtained using meteorological data at seven sites, the method was described in detail by Ishikawa *et al.* (1997).

We estimated the water balance for three periods: period I is the dry snow season (November to March), period II is the snowmelt season (April to May), and period III is the snow-free season (June to October). Water balance of each period and the whole year are summarized in Fig. 10 and Table 3. Solid precipitation was 53% of the total annual precipitation. In the deep snow pack region snowmelt occurs at the bottom of the snow cover even when the air temperature is far below the freezing point. Motoyama (1986) estimated bottom-melt by using air temperature and snow depth, and showed the contribution of bottom-melt to the runoff during the dry snow season. In this investigation the bottom-melt comprised about 30% of the winter runoff. However, winter runoff was much larger than the bottom-melt, which means there was discharge of the groundwater storage. During the snowmelt period the runoff became larger, about 45% of the annual runoff and 75% of the total snowmelt. Water loss due to evaporation was very small during the snowy season but became larger during summer and reached 44% of the total precipitation. Large evaporation of intercepted snow by dense coniferous canopies in midwinter was reported (Pomeroy and Gray 1995; Nakai *et al.* 1996). Therefore the interception should be estimated for the water balance of the experimental watershed. We have dealt with the winter precipitation as the amount of snow-water-equivalent (*SWE*) of the snow pack just before snowmelt, and the interception by tree canopies was not taken into account in the water balance. The total winter precipitation could be different from *SWE*, however, we assumed the difference was small because more than 70% of the watershed was sparse forest and open area.

Downloaded from http://iwaponline.com/hr/article-pdf/29/4-5/347/4827/347.pdf
by guest

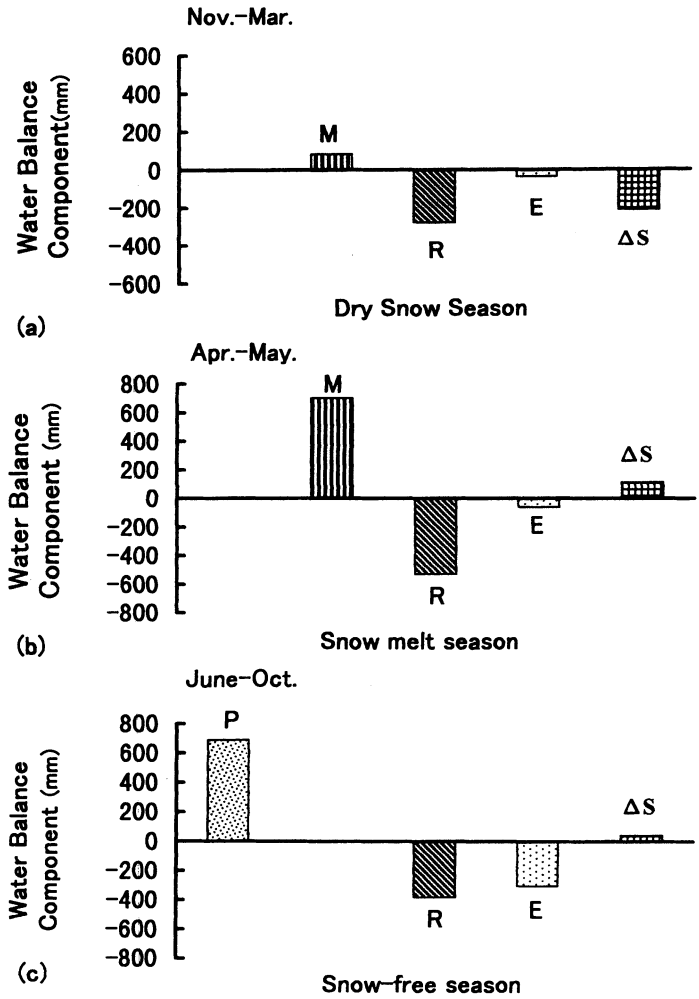

Fig. 10. Water balance at three different periods *P*: precipitation, *R*: runoff, *E*: evaporation, ΔS: change of ground water storage, (a):dry snow season, (b):snowmelt season (c):snow-free season

Table 3 – Water balance of the watershed at different periods

	Input		output		balance
Period	P(mm)	M(mm)	R(mm)	E(mm)	ΔS(mm)
I: Nov.-Mar.		84	-280	-15	-211
II: Apr.-May		705	-530	-60	115
III:Jun.-Oct.	690		-380	-305	5
whole year	690	789	-1190	-380	-91

Downloaded from http://iwaponline.com/hr/article-pdf/29/4-5/347/4827/347.pdf
by guest

Conclusion

Seasonal variations of water-balance components were measured at a small watershed in northern Hokkaido, Japan. In order to estimate the basin heat balance of snowmelt, the dependencies of meteorological parameters were examined. It was found that the net radiation and sensible heat flux increased with elevation because of a decrease in forest density, increase of wind speed, and temperature inversion. This resulted in an increasing snowmelt rate with elevation. The snowmelt at the bottom of the snow pack contributed about 30% of the runoff in winter. The snowmelt runoff occupied 45% of the total runoff and the runoff/snowmelt ratio was 0.75. Evaporation was negligibly small during the snowy season and markedly increased during the snow-free season. The water loss due to evaporation was half of the precipitation during summer, and the total loss was a quarter of the annual precipitation.

Acknowledgments

The authors express their sincere thanks to the staff of the Moshiri Branch of the Uryu Experimental Forest, Hokkaido University for their logistic support. Drs. D. Kobayashi, Inst. Low Temp. Sci., Hokkaido University and L. D. Hinzman, University of Alaska Fairbanks, provided useful comments and Ms. T. Kon'no made the figures for the manuscript. We also acknowledge the contributions of the two anonymous reviewers. A part of this research was supported by the scientific research fund from the Ministry of Education, Culture and Science of Japan.

References

Gray, D. M., and Landine, P. G. (1988) An energy-budget snowmelt model for Canadian prairies, *Canadian J. Earth Sci., Vol. 25(3)*, pp. 229-237.

Harding, R. J. (1986) Exchanges of energy and mass associated with a melting snowpack, International Association of Hydrological Sciences Publication, 155, pp. 3-15.

Ishikawa, N., Takeuchi, Y., Ishii, Y., and Kodama,Y. (1997) Characteristics of the water balance of the Moshiri Experimental watershed, *Annals of Glaciol., Vol. 25*, pp. 220-225.

Ishikawa, N., Nakatani, C., Kodama, Y., and Kobayashi, D. (1994a) Heat balance study on snowmelt in a small watershed, Seppyo, *J. Jpn, Soc. Snow and Ice, Vol. 56(1)*, pp. 31-43 (in Japanese).

Ishikawa, N., and Kodama, Y. (1994b) Transfer coefficients of sensible heat on a snowmelt surface, *Meteorology and Atmospheric Physics, Vol. 53,* pp. 233-240.

Ishikawa, N., Motoyama, H., and Kojima, K. (1986) Estimation of snow melting rates in a small experimental site, Proc. Cold Regions Hydrology Symposium, America Water Res. Assoc., pp. 305-312.

Downloaded from http://iwaponline.com/hr/article-pdf/29/4-5/347/4827/347.pdf
by guest

Koike, T., Takahashi, Y., and Yoshino, S. (1987) Modeling of snowmelt distribution for the estimation of basin-wide snowmelt using snow covered area. Large scale effects of seasonal snow cover, Proceedings of the Vancouver Symposium, August 1987, IAHS Publ., No. 166, pp. 192-212.

Male, D. H, and Granger, R. J. (1981) Snow surface energy exchange, *Water Resour. Res., Vol. 17*, pp. 609-627.

Motoyama, H. (1986) Studies on basin heat balance and snowmelt runoff models, Contr. Inst. Low Temp., Ser.A, 35, pp. 1-53.

Nakai, Y., Sakamoto, T., Terajima,T., and Kitamura, K. (1996) Evaporation of snow intercepted by a todo-fir forest. (II) Estimation by an energy balance model and their comparison with water balance measurements, *J. Jpn. Forest Soc., Vol. 78*, pp. 15-19.

Nakabayashi, H., Ishikawa, N., and Kodama,Y. (1996)Radiative Characteristics in forest during snowmelt season, Seppyo, *J. Jpn, Soc. Snow and Ice, Vol. 58(3)*, pp. 229-237 (in Japanese).

Ohta, T., Hashimoto,T., and Ishibashi, H. (1993) Energy budget comparison of snowmelt rates in a deciduous forest and an open site, *Annals of Glaciology, Vol. 18*, pp. 53-59.

Oke, T. R. (1987) *Boundary Layer Climate*, 2nd edn., Methuen; London, New York, 435 pp.

Pomeroy, J. W., and Grey, D. M. (1995)Snow cover: accumulation, relocation and Management, National Hydrology Research Institute, Science Report, No. 7, 144 pp.

Price, A. G., Dunne, T., and Colbeck, S. C. (1976) Energy balance and runoff from a subarctic snowpack, CRREL Report, Vol. 76 (27), pp. 1-29.

Received: November, 1997
Revised: April, 1998
Accepted: June, 1998

Address:
Institute of Low Temperature Science,
Hokkaido University,
N-19, W-8, Sapporo,
060 Japan.

Email: nobu@pop.lowtem.hokudai.ac.jp

Downloaded from http://iwaponline.com/hr/article-pdf/29/4-5/347/4827/347.pdf
by guest